Physicochemical Properties, Firmness, and Nanostructures of Sodium Carbonate-Soluble Pectin of 2 Chinese Cherry Cultivars at 2 Ripening Stages

LIFEN ZHANG, FUSHENG CHEN, HONGJIE AN, HONGSHUN YANG, XIAOYANG SUN, XINGFENG GUO, AND LITE LI

ABSTRACT: Firmness and physicochemical properties of 2 Chinese cherry (*Prunus pseudocerasus* L.) cultivars (soft cultivar "Caode" and crisp cultivar "Bende") at unripe and ripe stages were investigated, and the qualitative and quantitative information about sodium carbonate-soluble pectin (SSP) nanostructures was determined by atomic force microscopy (AFM). The lengths and widths of the cherry SSPs are very regular: almost all of the widths and lengths of SSP single molecules are composed of several basic units. The widths of the SSP chains are 37, 47, 55, and 61 nm, and the lengths are 123, 202, and 380 nm in both cultivars. The results show that the firmer cherry groups (crisp fruit) contain more percentages of wide and short SSP chains than soft fruit, and the unripe groups contain more percentages of wide and long SSP chains than corresponding ripe groups. They indicate that those nanostructural characteristics of SSP are closely related with firmness of the Chinese cherries in each cultivar.

Keywords: AFM, cherry, firmness, nanostructure, pectin, ripening

Introduction

Firmness is one of the most important quality indexes for fruits. It is essential to control a reasonable degree of softening of the fruit flesh to maintain a high marketing value. The mechanism by which fruits soften among ripening stages or cultivars is not fully illustrated. Changes of cell wall structures and compositions are considered to be the major factor of fruit softening (Ali and others 2004). Generally, softening of most fruit flesh is accompanied by changes in pectin structure. Fruit softening has been primarily attributed to solubilization of pectin in the middle lamella of cell walls (Ketsa and others 1999). Pectin changes occur in many ripening fruits; however, the degree of these changes is different among different fruits (Ali and others 2004).

Investigating the structural changes of pectin will be of benefit for illustrating the fundamentals of texture changes in different cultivars or ripening stages of fruits because pectin is a substantial source of texture in fruits. The correlation between flesh firmness and alkaline-soluble pectin of the cell wall polysaccharides is very high in 2 cultivars of pears (Murayama and others 2002). Therefore, the relationship between the firmness and nanostructures of alkaline-soluble pectin was investigated in this study.

Cherry is appreciated by most consumers for its nutrition and excellent quality (Martínez-Romero and others 2006; Vursavuş and others 2006). The physiochemical properties of cherry and microstructures were studied and it showed that softening is closely related to its quality assessment during postharvest (Yaman and Bayoındırlı 2002; Bernalte and others 2003; Tian and others 2004; Alonso and others 2005; Muskovics and others 2006). Softening is viewed as one of the main causes of cherry deterioration (Martínez-Romero and others 2006), and cherry during postharvest shows a general trend of firmness changes as most fruits do (Muskovics and others 2006; Vursavuş and others 2006). Therefore, cherry was selected as the study object.

Currently, nanotechnology receives a great deal of attention in food science. Atomic force microscopy (AFM), as one of the nanotechnology tools, has been applied to study fruit polysaccharides (Round and others 2001), pectin degradation during storage (Yang and others 2005b, 2006b, 2006c), starches (An and others 2008), food proteins (Yang and others 2007b), the morphology and surface structures of fruits (Yang and others 2005a), and food macromolecular manipulation (Yang and others 2006a). It offers both qualitative and quantitative results at nanoscale level without complex preparation of samples (Yang and others 2007a).

The objective of this study was to investigate the relationship between the physiochemical properties, firmness, and nanostructures of sodium carbonate-soluble pectin (SSP) in the fruit. Two Chinese cherry cultivars at different ripening stages were chosen for a comparative study. The nanostructures of Chinese cherry in different groups characterized by AFM show good correlation with physicochemical properties and firmness.

Materials and Methods

Fruit materials

Two Chinese cherry (*Prunus pseudocerasus* L.) cultivars (soft cultivar 'Caode' and crisp cultivar 'Bende') were used for the experiment. Two different stages (unripe and ripe) of maturity were applied and determined by experienced farmers. The ripe cherry was selected at commercial maturity stage, while the unripe cherry was about 7 d before ripe. The 2 cultivars were harvested by hand at a

MS 20070980 Submitted 12/29/2007, Accepted 2/18/2008. *Authors Zhang, Chen, Yang, Sun, Guo, and Li are with College of Food Science and Technology, Henan Univ. of Technology, Zhengzhou, Henan, 450052, P.R. China. Author An is with Teda Bio-X Center, College of Food Engineering and Biotechnology, Tianjin Univ. of Science & Technology, Tianjin, 300457, P.R. China. Direct inquiries to author Yang (E-mail: yhsfood@haut.edu.cn).*

doi: 10.1111/j.1750-3841.2008.00799.x

farm in Zhengzhou, Henan province, China. The fruits were transported to our laboratory within 2 h after harvest. Fruits with uniform size, disease free, and no other defects were selected. The 2 cultivars were named as soft cherry fruit and crisp cherry fruit according to their textural differences.

Firmness measurement

Fruit firmness was measured using a TA-XT2i texture analyzer (Stable Micro Systems Ltd., Godalming, Surrey, U.K.). Twenty fruits were measured without destruction for each sample. Whole cherries were used with skin and pit but without stem. A cylindrical probe with a diameter of 10 mm was used. The operating parameters were tested speed = 1.0 mm/s and pressed distance = 2.5 mm (Muskovics and others 2006).

Titratable acidity and total soluble solid content determination

The titratable acidity (TA), as percent malic acid, was determined by indicator titration with 0.1 M NaOH using 50 mL diluted juice (50 mL of pressed cherry juice were diluted to 250 mL with distilled water), and was terminated when the solution color changed into pink without fading in 30 s. The results were expressed as grams of malic acid equivalent to per 100 g^{-1} fruit weight (FW). Twenty fruits were chosen randomly for total soluble solids (TSS) content measurement of each lot. TSS content was determined with a digital refractometer (WYT-J, Sichuan, China) at 20 °C, and the results were expressed as °Brix (Bernalte and others 2003; Martínez-Romero and others 2006).

Cell wall preparation and SSP extraction and determination

Cell wall material of cherry flesh was extracted using the methods described by Deng and others (2005) with some modifications. Cherry flesh (10 g) was rapidly pestled in ice-cold mortar, then placed in 200 mL of 80% (v/v) boiling ethanol for 20 min. After being cooled to room temperature, the sample was filtrated with vacuum pump. The residue was re-extracted twice with ethanol, following the same experimental procedure. Subsequently, the residue was incubated overnight at 4 °C with 50 mL dimethysulphoxide (DMSO):water (9:1, v/v) to remove starch. Then, it was washed with water and transferred to 200 mL of chloroform:ethanol (2:1, v/v). After 10 min, the sample was filtrated and washed with 200 mL acetone until total whitening. Then the cell wall material was obtained. The cell wall material was suspended in 10 mL of 50 mM sodium acetate buffer (pH 6.5), agitated at 25 °C for 4 h, and then centrifuged at 10000 × *g* for 10 min at 4 °C. The residue was subjected to 2 additional 50 mM sodium acetate buffers. The water-insoluble pellet was resuspended in10 mL of 50 mM sodium acetate buffer (pH 6.5) containing 50 mM CDTA, shaken for 4 h, and centrifuged as described previously. The residue was further extracted twice with sodium acetate/CDTA, resuspended in 10 mL of 50 mM Na_2CO_3 containing 2 mM CDTA, shaken, and centrifuged as described previously. The supernatant was collected and the residue was re-extracted twice with Na_2CO_3/CDTA and centrifuged as described previously. All 3 supernatants were collected as the SSP.

The SSP content of Chinese cherry was determined by the Carbazole colorimetry method (Mu 2005). Galacturonic acid was used as standard. SSP solution (2 mL) was mixed with 12 mL of sulfuric acid (98%, w/w) in a test tube and cooled with ice water immediately, then boiled for 10 min and cooled with running tap water. Carbazole ethanol solution (0.5 mL) was added to the above-mentioned mixture system and the mixed solution was incubated at room temperature for 30 min, then the absorbance at 530 nm (A_{530nm}) was measured with a UV-2000 spectrophotometer (Unico Instrument Co. Ltd., Shanghai, China) at room temperature. The concentration of SSP solution can be diluted for obtaining a satisfactory result. All experiments were triplicated.

AFM determination

AFM determination was conducted according to the previous method with slight modifications (Yang and others 2005b, 2006b, 2006c). SSP solutions were diluted to a reasonable concentration or a series of concentrations. The diluted solutions were disrupted using a Vortex mixer (Fisher Scientific, Pittsburgh, Pa., U.S.A.). A small volume of the diluted solutions was pipetted onto mica surface, and then air-dried. The nanostructural characterization of SSP was performed using an AFM (JSPM-5200, JEOL, Japan) in AC mode. The NSC 11/no Al (MikroMasch, Wilsonville, Oreg., U.S.A.) tip with a resonance frequency of 330 KHz and a force constant of 48 N/m was used. All samples were measured in air (Yang and others 2007b).

AFM image analysis

The AFM images were analyzed offline with AFM software (WinSPM System, Tokyo, Japan). Flattening correction was applied to the images for obtaining high visual quality. The bright and dark areas in the images corresponded to peaks and troughs, respectively, as shown in height scale. Height mode images were analyzed, which included both 2-dimentional (plane) and 3-dimentional images. The quantitative data of the images were measured by section analysis. The characteristic dimensions (width, length, and height) of the samples can be obtained from section analysis (Yang and others 2007b).

Statistical analysis

Analysis of variance (ANOVA; $P < 0.05$) and Duncan's multiple range test for differences of different groups were carried out using SAS 9.1.3 software (SAS Inst. Inc., Cary, N.C., U.S.A.). Values of firmness, physicochemical properties, and AFM results were recorded as means ± standard deviations. Comparisons that yielded *P* values < 0.05 were considered significant. For AFM images, dozens of parallel images were analyzed for each specimen to obtain reliable and statistically valid results.

Results and Discussion

Effects of ripening stages and cultivars on the firmness and physicochemical properties of Chinese cherry

Table 1 shows firmness, TA, TSS, and contents of SSP in the 2 cultivars and 2 ripening stages. In both unripe and ripe groups, the firmness shows statistical differences between the 2 cultivars at a level of $P < 0.05$. Take ripe groups, for instance: the firmness of the soft cultivar is 233.1 g and the crisp cherry is 338.2 g. However, there are no statistical differences between ripe and unripe groups in the same cultivars. Firmness is one of the most important factors that affect the storage properties of fruits and vegetables. The decrease in firmness during ripening reflects cell enlargement during fruit growth. And the different rate of softening was characteristic of cultivars (Muskovics and others 2006).

The TA level of cherries varies among cultivars and is about 0.4% to 1.5%, of which the main organic acid is malic acid. TSS ranges from 11 and to 25 °Brix for most of the cherries and varies among cultivars as well (Martínez-Romero and others 2006). Our TA and TSS results are in these ranges. Compared to other cultivars, the TA and TSS of the 2 selected cultivars were closer to 'Noir De Guben,' '0-900 Ziraat' (Vursavuş and others 2006), than 'Van,' in

Turkey (Vursavuş and others 2006), 'Lapis' (Tian and others 2004), and 'StarKing' (Martínez-Romero and others 2006). The results reveal that the TA of the 2 cultivars decreased during cherry ripening (decreased to about 70% for both cultivars) but the TSS increased (Table 1). The 2 cultivars had similar changing patterns, which accords with many other reports (Martínez-Romero and others 2006; Muskovics and others 2006). The TA level decreased because the organic acid of fruits was consumed as substrate for respiration, and the TSS content increased because starch and other polysaccharides were hydrolyzed during fruit growth. The TSS contents are very close between the 2 cultivars (for unripe cherries, it is 10.8 for the soft and 11.0 for the crisp) but the TA contents vary in a large amount (for unripe cherries, it is 0.56 for the soft and 0.84 for the crisp).

The SSP content decreases with the ripening of cherry fruit (Table 1). During ripening, the SSP content decreases from 252.5 to 216.9 mg/100 g FW for the soft cultivar, and from 260.9 to 221.1 mg/100 g FW for the crisp fruit. For the same cultivar, higher content of SSP corresponds to higher firmness. The SSP contents of the crisp cherry fruits are slightly higher than those of the corresponding soft cherry fruit. However, the content of SSP and firmness are not consistent among different cultivars. Typically, pectins will be solubilized and sequentially disassembled through increased depolymerization of various pectin classes. In many fruits, increased solubility of pectins during ripening is attributed to the decreased contents of the SSP (Chin and others 1999; Ali and others 2004), which may also occur in this study.

Effects of ripening stages and cultivars on the qualitative and quantitative nanostructures of SSP

AFM images of Chinese cherry SSP in different groups are shown in Figure 1 to 3. The effects of ripening stages and cultivars on the nanostructure of SSP can be seen by comparing the images within these figures. The qualitative characteristics of the heterogeneous SSP structures, including cleavage point (cp), linear single fraction (ls), branching (br), and polymers (P), can be characterized

Table 1—Effects of ripening stages and cultivars on the firmness and physiochemical properties of Chinese cherries.

Group	SSP (mg·100 per gram FW)	TA (%)	TSS (°Brix)	Firmness (g)
Ripe soft fruit	216.9 ± 18.8^{c}	0.39 ± 0.02^{d}	13.3 ± 1.3^{a}	233.1 ± 31.6^{b}
Unripe soft fruit	252.5 ± 3.8^{ab}	0.56 ± 0.00^{c}	10.8 ± 1.2^{b}	236.2 ± 30.5^{b}
Ripe crisp fruit	221.1 ± 19.4^{bc}	0.59 ± 0.02^{b}	13.9 ± 1.3^{a}	338.2 ± 55.3^{a}
Unripe crisp fruit	260.9 ± 20.9^{a}	0.84 ± 0.00^{a}	11.0 ± 1.1^{b}	360.8 ± 51.0^{a}

SSP = sodium carbonate-soluble pectin; TA = titratable acidity; TSS = total soluble solids; Replicates (n): $n = 3$ for SSP; $n = 2$ for TA; and $n = 20$ for TSS and firmness.
Values in the same column with same superscript letters indicate no significant differences by the Duncan's multiple range test ($P < 0.05$).

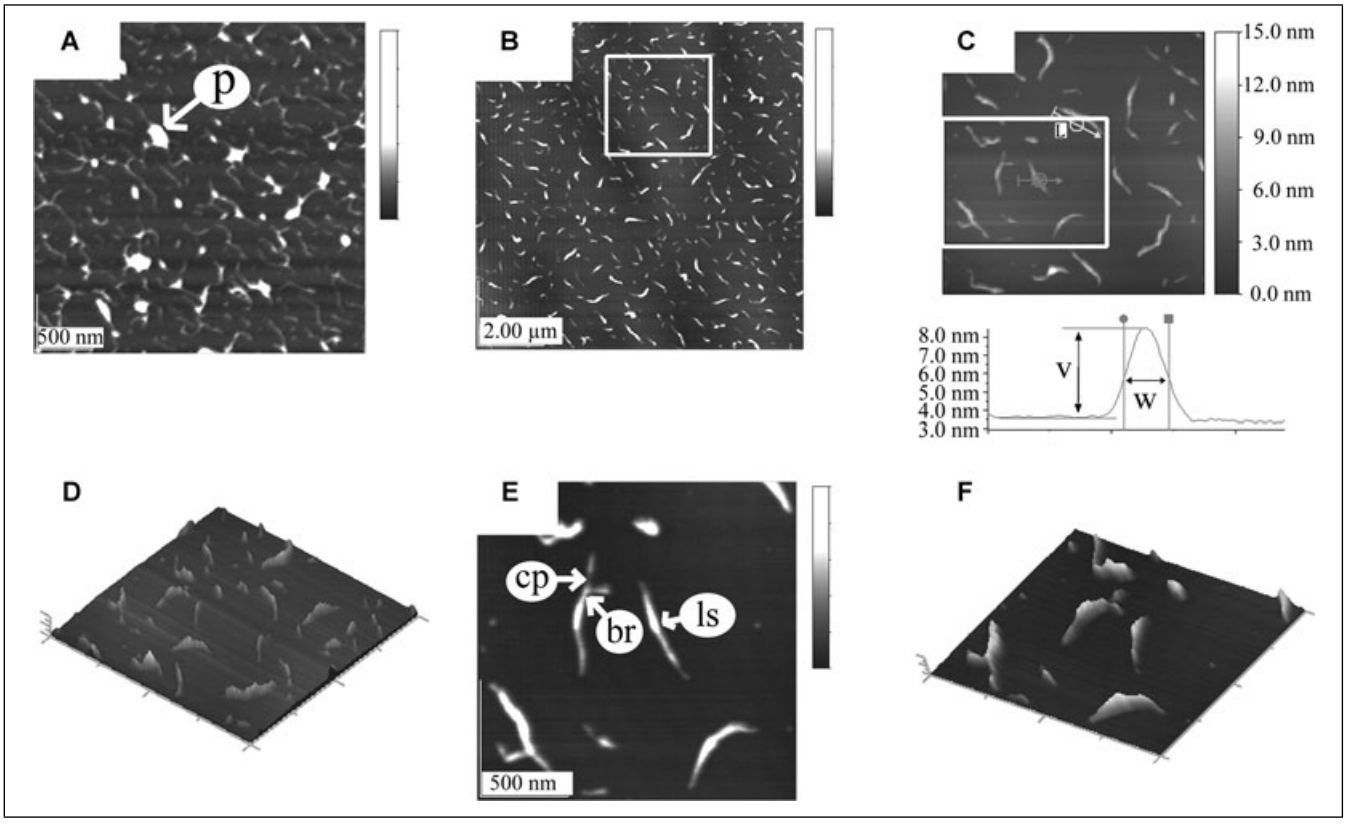

Figure 1—AFM images of SSP from soft ripe Chinese cherry. Height bar = 15 nm. (A) atypical image, scan area: 3.00 × 3.00 μm; (B) typical image, scan area: 10.00 × 10.00 μm; (C, D) zoom plane image in the marked region of (B) with section analysis and 3-dimensional image, scan area: 3.00 × 2.32 μm; (E, F) zoom plane image in the marked region of (C) and 3-dimensional images, scan area = 1.82 × 1.36 μm. Note: P = polymer; cp = cleavage point; br = branching; ls = linear single fraction.

by the high-resolution AFM images (Yang and others 2006b). The details of the images can be viewed more clearly through enlargement. For example, Figure 1C is the enlargement of the square part of Figure 1B. Three-dimensional images can also be obtained for better presentation of the results. For example, Figure 1D and 1F correspond to Figure 1C and 1E, respectively. Compared with ripe cherries, unripe cherries in both cultivars show more polymers that entangled together (Figure 2A, 2B, and 3E), while for ripe cherries, only few polymers or blocks can be seen in both cultivars (Figure 1A and 3A). Separate single linear chains are found more in both unripe groups; than ripe groups; the result is different from the structure of SSP molecules from fresh peach fruit (Yang and others 2006b).

AFM images can also reveal quantitative information of SSP in different groups. The color bar legends at the right of images denote the full height of the samples scanned, which can be used for determining the values in *z*-scale (height). In Figure 1 to 3, all *z*-range of these images is 15 nm. As shown in Figure 1C, the length, width, and the corresponding height of the SSP chains can be denoted by *L*, *W*, and *V*, respectively. Here, *V* means the height of SSP chains relative to the mica plane surface, *L* refers to the chain length, and Fq refers to the number of times that special chain widths or chain lengths occurred. Because the probe-broadening effect and side-by-side association of molecules may result in data imprecision, the peak width of chain half height (*W*) was applied to signify the chain width, which is different from the parameter we previously used for peach SSP (Yang and others 2006b), and the current value is about the half of the previous one. All the quantitative parameters of linear single fractions were analyzed by section analysis. A section analysis of SSP molecule is shown in Figure 1C.

Table 2 and 3 show the statistical results of SSP quantitative parameters. The 2 tables show that the chain widths (*W*) have limited discrete values. The widths of chains from section analysis reflect a group of basic units (37, 47, 55, and 61 nm), and the widths of other chains can be composed of these 4 values in both cultivars (Table 2). For example, 76, 91, 110, and 121 nm are approximately twice the number of 37, 47, 55, and 61 nm, respectively. The number of 85 nm is approximately the sum of 37 and 47 nm, and 140 nm is the sum of 37, 47, and 55 nm. Throughout the experiments, only 1 width of 69 nm cannot be explained by the 4 units. The widths of the cherries here are larger than those of orange albedo (Fishman and others 2007), but are comparable to those of peach (Yang and others 2006b). The chain lengths from section analysis also reflect a group of basic units in both cultivars (123, 202, and 380 nm), and the lengths of other chains can be composed of these 3 units as well (Table 3). For example, 324 nm is approximately the sum of 123 and 202 nm, and 529 nm is approximately the sum of one 123 nm and two 202 nm. However, 749 nm cannot be composed of the 3 basic units. The lengths of the SSP are longer than those from orange albedo (Fishman and others 2007). The heights (*V*) of the SSP of the cherries vary from 1.3 to 6.8 nm, mainly between 3 and 6 nm (Table 2), which is comparable to other pectins; for example, the heights of pectins from peach are about 1 to 2 nm (Yang and others 2006b, 2006c), about 0.5 nm for orange albedo (Fishman and others 2007), and 0.5 to 0.7 nm for tomato (Round and others 2001).

Table 2 and 3 show that crisp fruit contains more percentages of wide chain (from *W* value) and less percentages of long chain (from *L* value) than soft fruit in both ripening stages, respectively. For both cultivars, unripe groups contain more percentages of wide and long chains than ripe groups. There is no significant difference for the *V* values among all groups.

It should be noted that chains or polymers that are too small to be visualized precisely by the software were not used for the statistical analysis. The linear chain can be stretched after certain manipulation (Yang and others 2006a). However, SSP molecules, as

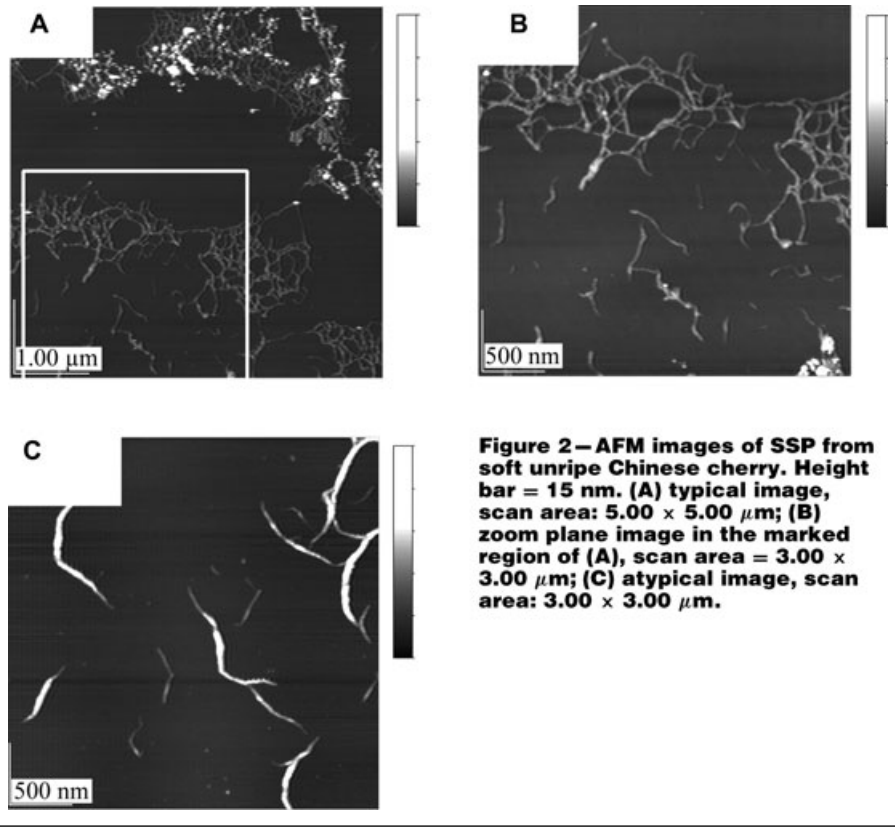

Figure 2—AFM images of SSP from soft unripe Chinese cherry. Height bar = 15 nm. (A) typical image, scan area: 5.00 × 5.00 μm; (B) zoom plane image in the marked region of (A), scan area = 3.00 × 3.00 μm; (C) atypical image, scan area: 3.00 × 3.00 μm.

natural macromolecules, tend to tangle with each other. We did not manipulate the SSP for illustrating the natural nanostructural information. The very regular widths and lengths of the SSP chains indicate that the SSP chains of Chinese cherries might be parallel linkage structures as native cellulose (Pérez and others 2000) and peach pectins (Yang and others 2005b, 2006b, 2006c). It was reported that depolymerization or shortening of chain length of pectin substances occurs with an increase of pectinesterase and

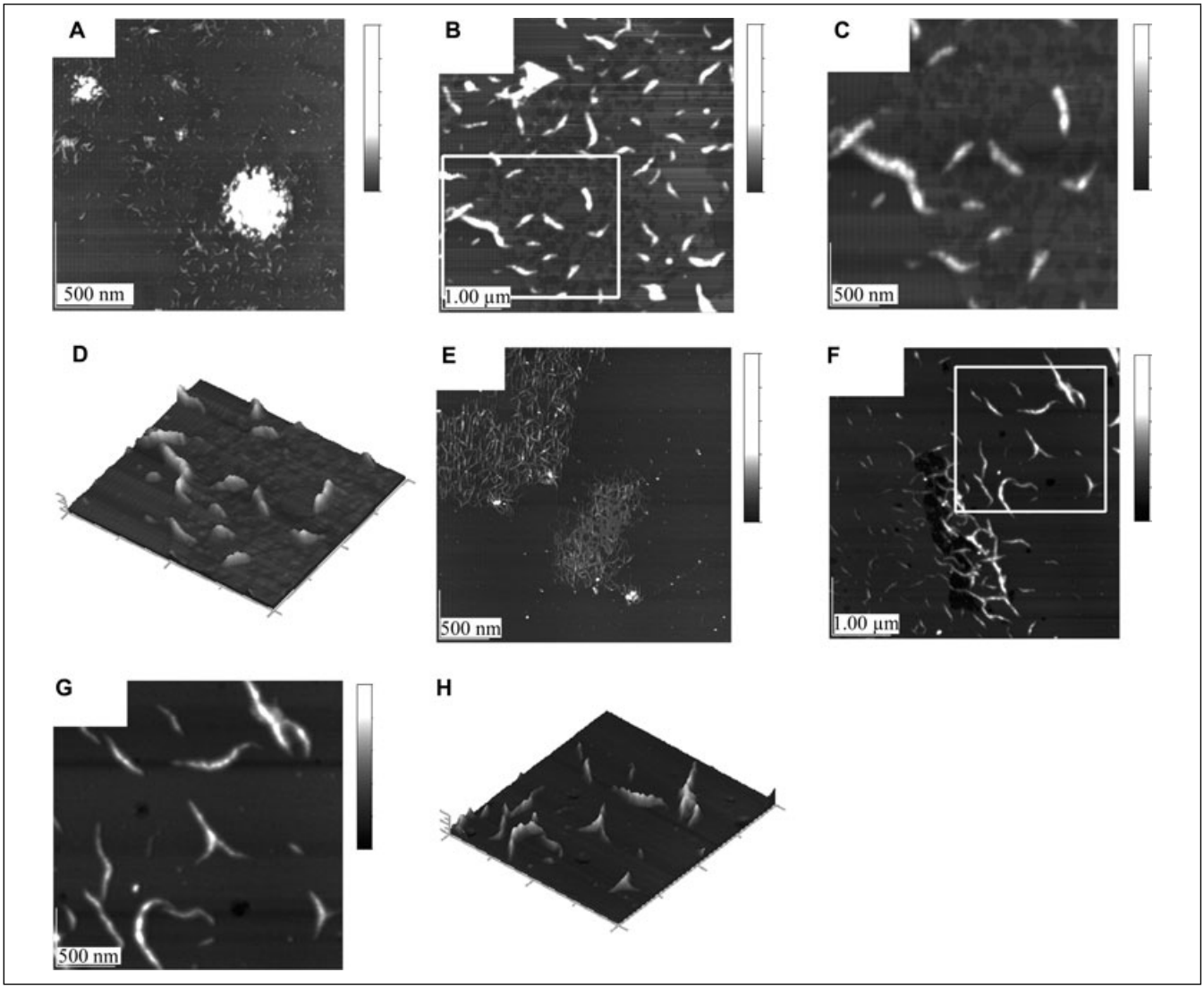

Figure 3—AFM images of SSP from ripe and unripe crisp Chinese cherry. Height bar = 15 nm. (A) atypical image, scan area: 19.30 × 17.10 μm; (B) typical image, scan area: 5.00 × 5.00 μm; (C, D) zoom plane image in the marked region of (B) and 3-dimensional image, scan area: 3.00 × 2.32 μm; (E) typical image, scan area: 3.00 × 3.00 μm; (F) atypical image, scan area: 5.00 × 5.00 μm; (G, H) zoom plane image in the marked region of (F) and 3-dimensional image, scan area: 2.63 × 2.91 μm. Note: A, B, C, D: ripe; E, F, G, H: unripe.

Table 2—Frequency and vertical distances of chain widths of Chinese cherry SSPs.

W	Ripe soft fruit		Unripe soft fruit		Ripe crisp fruit		Unripe crisp fruit	
(nm)	Fq	*V* (nm)	Fq	*V* (nm)	Fq	*V* (nm)	Fq	*V* (nm)
37	1	1.31 ± 0	3	1.15 ± 0.28	—	—	—	—
47	4	3.49 ± 0.55	2	1.98 ± 0.66	—	—	—	—
55	7	3.53 ± 0.99	5	2.88 ± 0.99	—	—	—	—
61	3	4.69 ± 0.98	3	3.09 ± 0.79	—	—	5	2.96 ± 0.20
69	1	3.81 ± 0	—	—	—	—	—	—
76	1	5.74 ± 0	4	5.25 ± 1.66	1	7.02 ± 0	2	3.05 ± 0.74
85	—	—	—	—	3	4.66 ± 1.69	4	6.74 ± 1.86
91	1	4.85 ± 0	3	6.89 ± 2.16	7	5.58 ± 1.18	3	3.23 ± 1.28
110	—	—	—	—	5	6.81 ± 1.09	3	1.61 ± 0.27
121	—	—	—	—	5	6.39 ± 1.08	4	2.80 ± 2.10
140	—	—	—	—	2	5.97 ± 1.40	4	2.73 ± 1.36

SSP = sodium carbonate-soluble pectin; *W* = the peak width of half height of SSP chains; *V* = the height of SSP chains; Fq refers to the numbers of times particular chain widths were observed.

Table 3—Frequency and chain lengths of Chinese cherry SSPs.

L (nm)	Ripe soft fruit		Unripe soft fruit		Ripe crisp fruit		Unripe crisp fruit	
	Fq	*L* ± SD (nm)	Fq	*L* ± SD (nm)	Fq	*L* ± SD (nm)	Fq	*L* ± SD (nm)
123	2	123 ± 4	—	—	—	—	1	123 ± 0
202	5	202 ± 23	—	—	6	202 ± 17	—	—
324	1	324 ± 0	—	—	5	324 ± 19	3	324 ± 45
380	—	—	—	—	5	380 ± 10	—	—
448	4	448 ± 16	1	448 ± 0	3	448 ± 20	1	448 ± 0
529	—	—	—	—	2	529 ± 4	—	—
573	—	—	1	573 ± 0	—	—	—	—
644	4	644 ± 1	2	644 ± 5	1	644 ± 0	—	—
749	1	749 ± 0	—	—	1	749 ± 0	3	749 ± 7
827	—	—	1	827 ± 0	—	—	—	—
1404	—	—	2	1404 ± 28	—	—	—	—

SSP = sodium carbonate-soluble pectin; *L* = lengths of SSP chains; Fq refers to the numbers of times particular chain lengths were observed. SD = standard deviation of the chain lengths.

polygalactronase activities (Yaman and Bayoındırlı 2002). Therefore, the changes of the SSP chains may strongly relate to the enzyme activity of cherry during ripening.

Relationship among firmness, physicochemical properties, and SSP nanostructure of cherries

Previous studies showed that there is a close relationship between firmness changes and the structures and contents of pectins (Chin and others 1999; Ketsa and others 1999; Murayama and others 2002; Ali and others 2004; Alonso and others 2005), especially between firmness and the content of SSP (Murayama and others 2002). Table 1 to 3 show that the firmness of crisp cherries is higher than that of soft cherries for both ripe and unripe groups. And the corresponding values of widths and lengths of the SSP are larger and smaller in crisp groups than those in soft groups, which demonstrates that the nanostructures of the SSP are closely related to the firmness between storage stages in each cultivar. Further research should be performed to examine the relationships in other fruits and vegetables.

Conclusions

Firmness, TA and TSS contents, and SSP nanostructures of soft and crisp Chinese cherry cultivars at unripe and ripe stages were determined to illustrate the fundamentals of the quality difference of fruits. The lengths and widths of the cherry SSPs are very regular; almost all of the widths and lengths of SSP single molecules are composed of several basic units in both cultivars (37, 47, 55, and 61 nm for width and 123, 202, and 380 nm for length). The results indicate that the firmer cherry group (crisp fruit) contained more percentages of wide and short SSP chains than soft fruit, and the unripe groups contained more percentages of wide and long SSP chains than the corresponding ripe groups.

Acknowledgments

Project 30600420 supported by National Natural Science Foundation of China contributed to this study. We also thank the financial support (nr 0200082) from Tianjin Univ. of Science and Technology.

References

Ali ZM, Chin LH, Lazan H. 2004. A comparative study on wall degrading enzymes, pectin modifications and softening during ripening of selected tropical fruits. Plant Sci 167:317–27.

Alonso J, Tortosa ME, Canet W, Rodriguez MT. 2005. Ultrastructural and changes in pectin composition of sweet cherry from the application of prefreezing treatments. J Food Sci 70:E526–30.

An H, Yang H, Liu Z, Zhang Z. 2008. Effects of heating modes and sources on nanostructure of gelatinized starch molecules using atomic force microscopy. LWT—Food Sci Technol, doi:10.1016/j.lwt.2007.08.026, Forthcoming.

Bernalte MJ, Sabio E, Hernández MT, Gervasini C. 2003. Influence of storage delay on quality of 'Van' sweet cherry. Postharvest Biol Technol 28:303–12.

Chin LH, Ali ZM, Lazan H. 1999. Cell wall modifications, degrading enzymes and softening of carambola fruit during ripening. J Exp Bot 50:767–75.

Deng Y, Wu Y, Li Y. 2005. Changes in firmness, cell wall composition and cell wall hydrolases of grapes stored in high oxygen atmospheres. Food Res Int 38:769–76.

Fishman ML, Cooke PH, Chau HK, Coffin DR, Hotchkiss AT. 2007. Global structures of high methoxyl pectin from solution and in gels. Biomacromolecules 8: 573–8.

Ketsa S, Chidtragool S, Klein JD, Lurie S. 1999. Firmness, pectin components and cell wall hydrolases of mango fruit following low-temperature stress. J Hortic Sci Biotech 74:685–9.

Martínez-Romero D, Alburquerque N, Valverde JM, Guillén F, Castillo S, Valero D, Serrano M. 2006. Postharvest sweet cherry quality and safety maintenance by *Aloe vera* treatment: a new edible coating. Postharvest Biol Technol 39:93–100.

Mu H. 2005. Food analytical technology. Beijing, China: Chemical Industry Press. p 79–83.

Murayama H, Katsumata T, Horiuchi O, Fukushima T. 2002. Relationship between fruit softening and cell wall polysaccharides in pears after different storage periods. Postharvest Biol Technol 26:15–21.

Muskovics G, Felföldi J, Kovács E, Perlaki R, Kállay T. 2006. Changes in physical properties during fruit ripening of Hungarian sweet cherry (*Prunus avium* L.) cultivars. Postharvest Biol Technol 40:56–63.

Pérez S, Mazeau K, du Penhoat CH. 2000. The three-dimentional structures of the pectic polysaccharides. Plant Physiol Biochem 38:37–55.

Round AN, Rigby NM, MacDougall AJ, Ring SG, Morris VJ. 2001. Investigating the nature of branching in pectin by atomic force microscopy and carbohydrate analysis. Carbohyd Res 331:337–42.

Tian S, Jiang A, Xu Y, Wang Y. 2004. Responses of physiology and quality of sweet cherry fruit to different atmospheres in storage. Food Chem 87:43–9.

Vursavuş K, Kelebek H, Selli S. 2006. A study on some chemical and physico-mechanic properties of three sweet cherry varieties (*Prunus avium* L.) in Turkey. J Food Eng 74:568–75.

Yaman Ö, Bayoındırlı L. 2002. Effects of an edible coating and cold storage on shelf-life and quality of cherries. Lebensm Wiss Technol 35:146–50.

Yang H, An H, Feng G., Li Y. 2005a. Visualization and quantitative roughness analysis of peach skin by atomic force microscopy under storage. LWT—Food Sci Technol 38:571–7.

Yang H, An H, Feng G, Li Y, Lai S. 2005b. Atomic force microscopy of the water-soluble pectin of peaches during storage. Eur Food Res Technol 220:587–91.

Yang H, An H, Li Y. 2006a. Manipulate and stretch single pectin molecules with modified molecular combing and fluid fixation techniques. Eur Food Res Technol 223:78–82.

Yang H, Feng G, An H, Li Y. 2006b. Microstructure changes of sodium carbonate-soluble pectin of peach by AFM during controlled atmosphere storage. Food Chem 94:179–92.

Yang H, Lai S, An H, Li Y. 2006c. Atomic force microscopy study of the ultrastructural changes of chelate-soluble pectin in peaches under controlled atmosphere storage. Postharvest Biol Technol 39:75–83.

Yang H, Wang Y, Lai S, An H, Li Y, Chen F. 2007a. Application of atomic force microscopy as a nanotechnology tool in food science. J Food Sci 72:R65–75.

Yang H, Wang Y, Regenstein JM, Rouse DB. 2007b. Nanostructural characterization of catfish skin gelatin using atomic force microscopy. J Food Sci 72:C430–40.